

Spin pumping effect in non-Fermi liquid metals

Xiao-Tian Zhang,¹ Yuya Ominato,^{1,2} Long Zhang,¹ and Mamoru Matsuo^{1,3,4}

¹*Kavli Institute for Theoretical Sciences and CAS Center for Excellence in Topological Quantum Computation, University of Chinese Academy of Sciences, Beijing 100190, China*

²*Waseda Institute for Advanced Study, Waseda University, Shinjuku, Tokyo 169-8050, Japan.*

³*RIKEN Center for Emergent Matter Science (CEMS), Wako, Saitama 351-0198, Japan*

⁴*Advanced Science Research Center, Japan Atomic Energy Agency, Tokai, 319-1195, Japan*

(Dated: August 7, 2023)

We propose that the spin pumping effect is a valuable probe to non-Fermi liquid (NFL) metals in correlated electron systems. In a bilayer structure composed of a NFL metal and a ferromagnetic insulator subjected to ac magnetic field, the precessing spins in the FI inject spin current into the NFL metal, which modulates the ferromagnetic resonance (FMR) as a backaction. For NFL metals in the vicinity of a quantum critical point, the FMR modulation shows power-law scaling with the frequency and the temperature, which is closely related to the quantum critical behavior and reflects the non-quasiparticle nature of spin relaxation in NFL metals.

Introduction.—The breakdown of coherent Fermi-liquid quasiparticles is the most dramatic manifestation of the many-body interaction effect in strongly correlated electron systems, which is dubbed the non-Fermi liquid (NFL) behavior. Coherent quasiparticles can be destroyed by coupling to critical fluctuations of order parameters in the vicinity of quantum critical points (QCPs) [1, 2], where physical quantities exhibit universal scaling form in the quantum critical regime distinct from the Fermi liquid metals. Evidence of NFL behavior has accumulated mainly from electric transport experiments in cuprate superconductors [3, 4], and heavy-fermion compounds [5], etc. More diagnostics of the NFL state is greatly desired.

Recently, vigorous studies have been conducted on spin pumping, the transfer of spin angular momentum from the dynamics of magnetization driven by ferromagnetic resonance (FMR) to an adjacent material on a magnet [6, 7]. The spin pumping, at a microscopic level, is initiated by the magnetic exchange interaction at the interface between the magnetization in the magnet and the electron spin in the adjacent material [8–10]. This interaction leads to spin injection into the material and generates a self-energy of the magnons in the magnet as a backaction, modulating the frequency of FMR and Gilbert damping [11, 12]. The modulated FMR signal carries information about the dynamical spin susceptibility of the thin-film material attached to the ferromagnet, making it a useful probe for studying its spin characteristics [13]. The effectiveness of spin pumping as a sensitive probe, demonstrated by its use in measuring the magnetic phase transition in an antiferromagnetic ultra-thin film [14], shows its potential as a quantum probe in complex systems beyond simple quasiparticle models. This implies vast research potential in using spin pumping effect to explore spin properties in strongly correlated electron systems, including detecting the pairing symmetry in superconductors [12, 15].

In this Letter, we study the spin pumping effect in

the bilayer system composed of a NFL metal and a ferromagnetic insulator (FI) thin film schematically shown in Fig. 1. The injected spin current is carried by “non-quasiparticles” in the NFL metal. We focus on NFL metals induced in the quantum critical regime of QCPs and take the two-dimensional (2D) Ising nematic QCP as a concrete example. The FMR frequency and the Gilbert damping coefficient are significantly modulated by the spin pumping into the NFL metal at both zero and finite temperatures. The FMR modulation shows power-law scaling with frequency and temperature, which are closely related to the universal critical exponents of the QCP. Therefore, the FMR-driven spin pumping is a valuable probe to the NFL metals in strongly correlated electron systems.

We start with a generic relation between the FMR modulation and the dynamical spin susceptibility in NFL metals. Then, we calculate the FMR modulation of the NFL metal close to the 2D Ising nematic QCP at both zero and finite temperature, highlighting the power-law scaling with frequency and temperature. We hope this work can motivate further study of NFL metals and other strongly correlated electron systems from the spintronics perspective in the future.

FMR modulation in NFL metals.—Let us consider the bilayer structure composed of a NFL metal and a FI thin film shown in Fig. 1. The FI is driven by an external ac magnetic field in resonance with the precession of local spins. The spin current is injected into the NFL metal via the exchange coupling at the interface. The backaction modulates the FMR frequency and the Gilbert damping coefficient, which can be measured in experiments. The full Hamiltonian of the NFL/FI bilayer comprises three parts,

$$\mathcal{H}(t) = \mathcal{H}_{\text{FI}}(t) + \mathcal{H}_{\text{ex}} + \mathcal{H}_{\text{NFL}} \quad (1)$$

The first term describes the FI with the ferromagnetic Heisenberg model subjected to an oscillating magnetic

field,

$$\begin{aligned} \mathcal{H}_{\text{FI}}(t) = & -J \sum_{\langle i,j \rangle} \mathbf{S}_i \cdot \mathbf{S}_j + \gamma_g H \sum_i S_i^z \\ & - \gamma h_{\text{ac}} \sum_i (S_i^x \cos \omega t - S_i^y \sin \omega t), \end{aligned} \quad (2)$$

in which $J > 0$ is the ferromagnetic exchange coupling constant. \mathbf{S}_i stands for the local spin at site i in the FI. H is the magnitude of the Zeeman field. γ_g (< 0) is the gyromagnetic ratio. h_{ac} and ω are the amplitude and the frequency of the circularly oscillating external magnetic field, respectively. The second term in Eq. (1) is the exchange coupling at the interface between local spins in the FI and itinerant electrons in the NFL metal,

$$\mathcal{H}_{\text{ex}} = \sum_i \int d^2r J(\mathbf{r}, \mathbf{r}_i) \mathbf{S}_i \cdot \mathbf{s}(\mathbf{r}), \quad (3)$$

where $\mathbf{s}(\mathbf{r}) = \frac{1}{2} c_{\alpha}^{\dagger}(\mathbf{r}) \boldsymbol{\sigma}_{\alpha\beta} c_{\beta}(\mathbf{r})$ is the itinerant electron spin operator. The spin-flip terms in the exchange coupling can be written in the reciprocal space as $\mathcal{H}_{\text{flip}} = \sum_{\mathbf{k}, \mathbf{q}} (J_{\mathbf{k}, \mathbf{q}} s_{\mathbf{q}}^{+} S_{\mathbf{k}}^{-} + \text{H.c.})$. The exchange coupling function in the reciprocal space is approximately given by

$$|J_{\mathbf{k}, \mathbf{q}}|^2 = \frac{J_1^2}{N} \delta_{\mathbf{k}, \mathbf{q}} + \frac{J_2^2 l^2}{AN}, \quad (4)$$

in which A is the area of the interface, and l is the spatial correlation length of quenched disorders at the interface. J_1 and J_2 are related to the mean value and the variance of the exchange coupling [12].

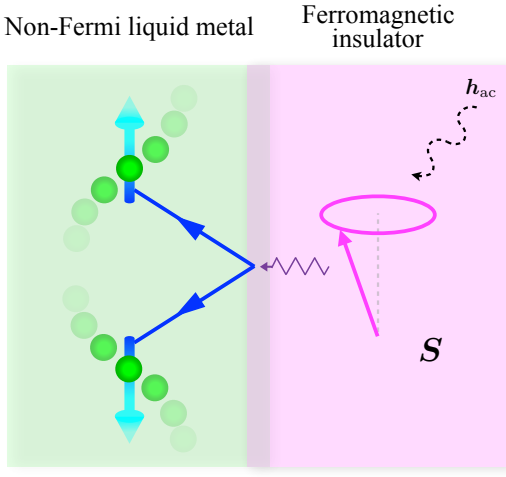


FIG. 1. Schematic plot of the NFL/FI bilayer structure for the FMR-driven spin pumping experiment. The pink arrow in the FI indicates the spin \mathbf{S} precessing in the external ac magnetic field \mathbf{h}_{ac} . The blue arrows in the NFL metal indicate the itinerant electrons exchanging spin angular momentum at the interface with magnons in the FI layer. The gradually fainted green balls illustrate the incoherent quasiparticles in the NFL metal.

Let us consider the NFL metals induced by coupling electrons c_{α} ($\alpha = \uparrow, \downarrow$) to a critical fluctuating order parameter field $\phi(\mathbf{r})$. The third term in Eq. (1) denotes the following generic form,

$$\begin{aligned} \mathcal{H}_{\text{NFL}} = & \int d^2r \left[c_{\alpha}^{\dagger}(\mathbf{r}) \epsilon(-i\partial_{\mathbf{r}}) c_{\alpha}(\mathbf{r}) - \lambda O(\mathbf{r}) \phi(\mathbf{r}) \right. \\ & \left. + \frac{1}{2} (\partial_{\mathbf{r}} \phi)^2 + \frac{r}{2} \phi^2 \right], \end{aligned} \quad (5)$$

in which $\epsilon(\mathbf{k})$ is the bare electron dispersion, λ is the coupling constant of electrons and the order parameter field $\phi(\mathbf{k})$, and r is the tuning parameter towards the QCP. $O(\mathbf{r})$ is a fermion bilinear operator, which transforms inversely as $\phi(\mathbf{r})$ under symmetry actions guaranteeing the invariance of the coupling term.

The backaction of the spin pumping renormalizes the magnon Green's function in the FI [8, 9], which is calculated from the Feynman diagram shown in Fig. 2 (a). The retarded magnon Green's function takes the following form,

$$G(\mathbf{k}, \omega) = (\omega - \omega_{\mathbf{k}} + i\alpha\omega - \Sigma(\mathbf{k}, \omega))^{-1}, \quad (6)$$

in which the bare magnon dispersion reads $\omega_{\mathbf{k}} = Dk^2 - \gamma_g H$, and $\Sigma(\mathbf{k}, \omega)$ is the magnon self-energy due to the backaction of the spin pumping. In a generic bosonic system, the self-energy has an imaginary part proportional to ω [16], and the coefficient α is called the Gilbert damping constant [6]. The FMR modulation is determined by the uniform component ($\mathbf{k} = 0$) of the magnon Green's function, in which the pole dictates the resonance condition, $\omega + \gamma_g H - \text{Re}\Sigma_{\mathbf{k}=0}(\omega) = 0$, thus the resonance frequency is shifted by $\delta H = \gamma_g^{-1} \text{Re}\Sigma_{\mathbf{k}=0}(\omega)$. The imaginary part of the self-energy leads to an enhanced Gilbert damping coefficient, $\delta\alpha = -\omega^{-1} \text{Im}\Sigma_{\mathbf{k}=0}(\omega)$.

The magnon self-energy can be calculated perturbatively in terms of the external oscillating magnetic field h_{ac} and the exchange coupling $J_{\mathbf{k}, \mathbf{q}}$ [8, 10],

$$\Sigma(\mathbf{k}, \omega) = - \sum_{\mathbf{q}} |J_{\mathbf{k}, \mathbf{q}}|^2 \chi(\mathbf{q}, \omega), \quad (7)$$

with $\chi(\mathbf{q}, \omega) \equiv i \int dt e^{i(\omega+i\omega^+)} \Theta(t) \langle [s_{\mathbf{q}}^{+}(t), s_{-\mathbf{q}}^{-}(0)] \rangle$ being the retarded dynamical spin susceptibility for NFL metals. Inserting the exchange coupling function in Eq. (4), the magnon self-energy is given by [12]

$$\Sigma_{\mathbf{k}=0}(\omega) = -\frac{J_1^2}{N} \chi_{\text{uni}}(\omega) - \frac{J_2^2 l^2}{AN} \chi_{\text{loc}}(\omega). \quad (8)$$

Here, the uniform and the local components of the dynamical spin susceptibility, defined by $\chi_{\text{uni}}(\omega) = \chi(\mathbf{q} = 0, \omega)$ and $\chi_{\text{loc}}(\omega) = \sum_{\mathbf{q}} \chi(\mathbf{q}, \omega)$, dominate in opposite limits set by the ratio $J_1 \sqrt{A}/(J_2 l)$.

In the vicinity of the QCP at $r = r_c$, the dynamical spin susceptibility takes the following universal scaling form at zero temperature, $\chi(\mathbf{q}, \omega, r - r_c) = \xi^d \chi(\mathbf{q}\xi, \omega\xi^z)$,

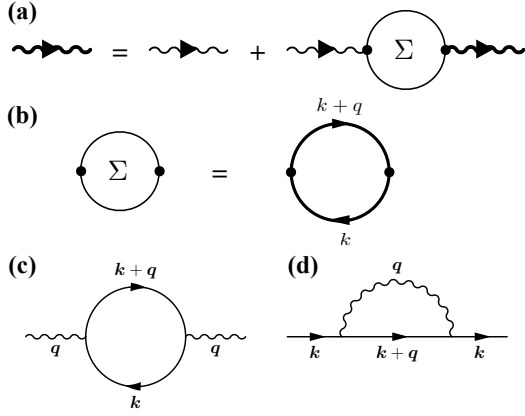


FIG. 2. Feynman diagrams for perturbative calculations. (a) Dyson equation for the magnon Green's function. The thin and the thick wavy lines are the bare and the renormalized magnon Green's functions, respectively. The circle stands for the magnon self-energy Σ . (b) The magnon self-energy is equivalent to the dynamical spin susceptibility of the NFL metal, which can be calculated with the renormalized electron propagator (thick lines) up to one-loop order. (c-d) One-loop corrections to (c) the boson polarization function and (d) the electron self-energy in the NFL metal. The straight and the wavy lines are the electron and the boson propagators, respectively.

in which ξ is the spatial correlation length, d_χ is the scaling dimension of the spin susceptibility, and z is the dynamical exponent. At the QCP, the correlation length diverges, leading to the reduced scaling form, $\chi(\mathbf{q}, \omega, 0) = \omega^{-d_\chi/z} \tilde{\chi}(\mathbf{q}/\omega^{1/z})$. Therefore, the uniform and the local components show different power-law scaling forms with the frequency,

$$\chi_{\text{uni}}(\omega) \sim \omega^{-d_\chi/z}, \quad \chi_{\text{loc}}(\omega) \sim \omega^{(2-d_\chi)/z}. \quad (9)$$

The critical exponents d_χ and z can be extracted from their contributions to the resonance frequency shift and the enhanced Gilbert damping coefficient. The power-law scaling with the frequency is in sharp contrast to the conventional Gilbert damping mechanism, thus reflects the NFL nature at the QCP.

The quantum critical regime extends to nonzero temperatures above the QCP, where a different set of critical exponents d'_χ and z' may emerge in the following scaling form,

$$\chi(\mathbf{q}, \omega, r - r_c, T) = L_\tau^{d'_\chi/z'} \chi(\mathbf{q} L_\tau^{1/z'}, \omega L_\tau, \xi(T)/L_\tau^{1/z'}). \quad (10)$$

Here, $L_\tau = 1/(k_B T)$ is a characteristic scale in the imaginary time direction. Therefore, we have

$$\chi_{\text{uni}}(\omega, T) = T^{-d'_\chi/z'} \chi(\omega/T, \xi(T) T^{1/z'}), \quad (11)$$

$$\chi_{\text{loc}}(\omega, T) = T^{(d-d'_\chi)/z'} \tilde{\chi}(\omega/T, \xi(T) T^{1/z'}). \quad (12)$$

The frequency and temperature dependence of the FMR modulation in the quantum critical regime at finite temperature is also a characteristic feature of the NFL metal.

FMR modulation at 2D Ising nematic QCP.—Let us take the 2D Ising nematic QCP as a concrete example, which could be relevant to experiments in underdoped cuprates [4] and iron-based superconductors [17]. The order parameter field $\phi(\mathbf{r})$ changes sign under the four-fold lattice rotation transformation. The fermion bilinear operator $O(\mathbf{r})$ in Eq. (5) is given by

$$O(\mathbf{r}) = \frac{1}{A} \sum_{\mathbf{q}} \sum_{\mathbf{k}, \alpha} d_{\mathbf{k}} c_{\mathbf{k}-\mathbf{q}/2, \alpha}^\dagger c_{\mathbf{k}+\mathbf{q}/2, \alpha} e^{i\mathbf{q} \cdot \mathbf{r}}, \quad (13)$$

where $d_{\mathbf{k}} = \cos k_x - \cos k_y$ is the d -wave form factor. The four-fold lattice rotation symmetry is spontaneously broken in the Ising nematic ordered phase. Coherent quasiparticles are destroyed by critical fluctuations of the Ising nematic order parameter $\phi(\mathbf{r})$ in the quantum critical regime.

Let us consider the smooth NFL/FI interface for simplicity. In this case, $J_1 \gg J_2 l / \sqrt{A}$, thus the uniform component of the dynamical spin susceptibility $\chi_{\text{uni}}(\omega)$ dominates, which can be calculated up to one-loop order as [see Fig. 2 (b)]

$$\chi(\omega) = i \sum_{\alpha\beta} \sigma_{\alpha\beta}^+ \sigma_{\beta\alpha}^- \sum_{\mathbf{k}} \int \frac{d\omega'}{2\pi} g_\alpha(\mathbf{k}, \omega') g_\beta(\mathbf{k}, \omega' + \omega). \quad (14)$$

Here, the renormalized fermion propagator of the NFL metal is defined by $g_\alpha(\mathbf{k}, \omega + i0^+) = -i \int d\tau e^{i(\omega+i0^+)\tau} \langle \mathcal{T}_c c_{\mathbf{k}, \alpha}(\tau) c_{\mathbf{k}, \alpha}^\dagger(0) \rangle$ where \mathcal{T}_c is the time ordering on the Keldysh contour.

The NFL metal near the Ising nematic QCP can be captured by the patch theory [18, 19], in which the momenta near the Fermi surface are decomposed into patches $\mathbf{k} = \mathbf{k}_{F,s} + \delta\mathbf{k}$, in which s is the patch index, while $\mathbf{k}_{F,s}$ and $\delta\mathbf{k}$ are the Fermi momentum and a small deviation at the s -th patch, respectively. Denoting the radial and the tangential components of $\delta\mathbf{k}$ by δk_x and δk_y , the bare electron propagator is given by $g_s^0(\mathbf{k}, \omega + i0^+) = (\omega + i0^+ - v_F \delta k_x - \kappa \delta k_y^2/2)^{-1}$. The boson polarization is induced by the electron-hole excitations near the Fermi surface captured by Fig. 2 (c) up to one-loop order, which yields $-ic_B \omega / |q_y|$. The renormalized boson propagator is then adopted to calculate the electron self-energy [see Fig. 2 (d)] in the same spirit as the Hertz-Millis theory of ferromagnetic metals [20, 21]. The dynamically generated electron self-energy overwhelms the bare kinetic term in the low-energy limit $\Sigma_e(\mathbf{k}_F, \omega) \sim -d_{\mathbf{k}_F}^2 |\omega|^{2/3} (\text{sgn}(\omega) + i/\sqrt{3})$. The NFL nature is captured by the vanishing quasiparticle weight in the $\omega \rightarrow 0^+$ limit for $k_{F,x} \neq \pm k_{F,y}$: $Z_{\mathbf{k}_F}(\omega) = (1 - \partial_\omega \text{Re} \Sigma_e(\mathbf{k}_F, \omega))^{-1} \sim d_{\mathbf{k}_F}^{-2} \omega^{1/3}$. The renormalized electron propagator is given by [22]

$$g_s(\mathbf{k}, k_0) = (ic_F d_{\mathbf{k}_{F,s}}^2 |\omega|^{2/3} - v_F k_x - \kappa k_y^2/2)^{-1} \quad (15)$$

for $\omega < \omega_c = c_F^3$ with $c_F = \lambda^2 / (\sqrt{3} \pi v_F c_B^{1/3})$. The dy-

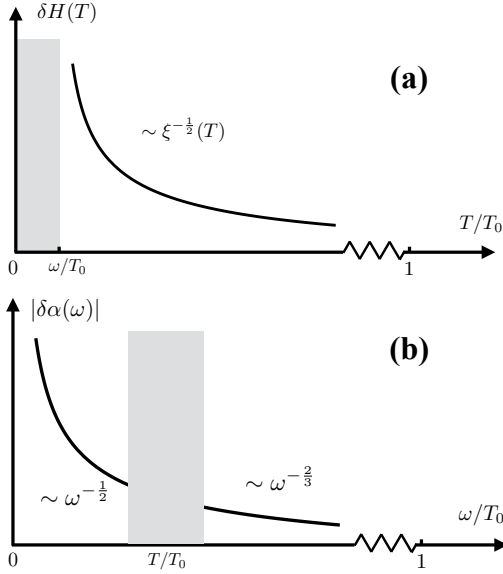


FIG. 3. Schematic illustrations of the FMR modulations scaling forms. The frequency and temperature are rescaled by a characteristic temperature T_0 ($\gg T$). (a) Temperature dependence of the resonance frequency shift $\delta H(T)$. The finite temperature ($T > \omega$) $\delta H(T)$ shows a rapid increase approaching low- T owing to the divergent correlation length. (b) Frequency dependence of the enhanced Gilbert damping coefficient $|\delta\alpha(\omega)|$. The magnitude of $\delta\alpha$ displays different scaling forms in the low-frequency ($\omega < T$, left) and high-frequency ($\omega > T$, right) regions.

nematical exponent $z = 3$ is not modified until the three-loop order [18].

The uniform spin susceptibility evaluated with Eq. (15) has a scaling dimension $d_\chi = d - z$. The retarded magnon self-energy is given by

$$\Sigma_{k=0}(\omega) = \frac{4\pi^2 J_1^2 \rho_F}{N} \left| \frac{\omega}{\omega_c} \right|^{1/3} \left[\sqrt{3} - i \text{sgn}(\omega) \right], \quad (16)$$

in which ρ_F is the density of states at the Fermi energy. The resonance frequency shift and the enhanced Gilbert damping have the following scaling forms in the low-energy limit,

$$\delta\alpha \sim |\omega|^{-2/3}, \quad \delta H \sim \gamma_g^{-1} |\omega|^{1/3}. \quad (17)$$

These are schematically plotted in Fig. 3. The diverging coefficient $\delta\alpha$ in the zero-frequency limit indicates a novel spin relaxation mechanism, which is in sharp contrast to the conventional Gilbert damping.

FMR modulation at finite temperature.—The finite-temperature properties of the NFL metal close to the Ising nematic QCP cannot be simply inferred from the zero-temperature results by assuming the ω/T scaling [23, 24]. It has been proposed based on the renormalization group calculations [25] that the boson dynamics at finite temperature is characterized by a dynamical exponent $z = 2$ instead of $z = 3$ at zero temperature, which

has been confirmed by quantum Monte Carlo simulations [26]. The renormalized boson and fermion propagators are given by [24],

$$g(\mathbf{k}, \omega + i0^+) = (\omega + i0^+ - \epsilon_{\mathbf{k}} + i\gamma_{\mathbf{k}_F}(T))^{-1}, \quad (18)$$

$$D(\mathbf{q}, \Omega + i0^+) = \left(\xi^{-2}(T) + a|\mathbf{q}|^2 - ib\frac{\Omega}{\gamma(T)} \right)^{-1}. \quad (19)$$

where a and b are nonuniversal constants. The correlation length $\xi(T)$ and the electron scattering rate $\gamma(T)$ scale as $\xi(T)^{-1} \sim \sqrt{T/\ln(\epsilon_F/T)}$ and $\gamma(T) \sim \sqrt{T/\ln(\epsilon_F/T)}$ in the quantum critical regime. The imaginary part of the retarded self-energy $\gamma_{\mathbf{k}_F}(T) = -\text{Im}\Sigma(\mathbf{k}_F, \omega = 0; T)$ is calculated in an asymptotic temperature range $T \ll T_0$, $\gamma_{\mathbf{k}_F}(T) = -(\lambda^2 d_{\mathbf{k}_{F,s}}^2)(4v_F\sqrt{a})T\xi(T)$, where the upper bound T_0 is specified by the condition $|\gamma_{\mathbf{k}_F}(T)|/v_F \ll \xi^{-1}(T)/\sqrt{a}$, thus $T_0 = \epsilon_F e^{-\lambda^2/v_F^2}$. These results are valid for $\omega < T \ll T_0 < \omega_c$, while the zero-temperature results presented before should be valid in the low-temperature regime for $T < \omega$.

The real part of the electron self-energy can be obtained from the Kramers-Krönig relation as $\text{Re}\Sigma_e(\mathbf{k}_F, \omega) \sim -d_{\mathbf{k}_F}\omega\xi(T)^{-1}$ for $|\omega| < T < \omega_c$. The quasiparticle weight given by

$$Z(\mathbf{k}_F, \omega; T) \simeq d_{\mathbf{k}_F}^{-2} \xi(T)^{-1}, \quad k_{F,x} \neq \pm k_{F,y}, \quad (20)$$

vanishes approaching the QCP due to the divergent $\xi(T)$.

The renormalized electron propagator in Eq. (18) is used to evaluate the dynamical spin susceptibility and the magnon self-energy at finite temperature, which yields

$$\Sigma_{k=0}(\omega) = \frac{\sqrt{2}\pi J_1^2 \rho_F}{N} \left(\frac{4}{\pi} \xi^{-\frac{1}{2}}(T) + i \text{sgn}(\omega) \sqrt{\frac{|\omega|}{\gamma(T)}} \right). \quad (21)$$

Accordingly, the FMR frequency shift and the enhanced Gilbert damping coefficient have the following scaling form

$$\delta\alpha \sim -(|\omega|\gamma(T))^{-\frac{1}{2}}, \quad \delta H \sim \gamma_g^{-1} \xi^{-\frac{1}{2}}(T), \quad (22)$$

which are schematically plotted in Fig. 3.

Summary.—We propose that the FMR-driven spin pumping effect in the NFL/FI bilayer structure is a valuable probe to the NFL metal. In the NFL metal close to an Ising nematic QCP, the resonance frequency shift and the enhanced Gilbert damping exhibit power-law scaling with frequency and temperature both at the QCP and in the finite- T quantum critical regime, which are closely related to the critical exponents. Therefore, the spintronics experiments can shed light on the non-quasiparticle nature of spin relaxation in the NFL metals.

This work is partially supported by China's Ministry of Science and Technology (Grant No. 2022YFA1403900) and National Natural Science Foundation of

China(NSFC) (Grant No. 11920101005). L.Z. is supported by the National Key R&D Program of China (Grant No. 2018YFA0305800), the NSFC (Grant No. 12174387), the Strategic Priority Research Program of CAS (Grant No. XDB28000000), and the CAS Youth Innovation Promotion Association. M.M. is supported by the Priority Program of Chinese Academy of Sciences under Grant No. XDB28000000, and by JSPS KAKENHI for Grants (Nos. 21H01800, and 21H04565, and 23H01839) from MEXT, Japan.

-
- [1] Hilbert v. Löhneysen, Achim Rosch, Matthias Vojta, and Peter Wölfle, “Fermi-liquid instabilities at magnetic quantum phase transitions,” Rev. Mod. Phys. **79**, 1015–1075 (2007).
 - [2] Sung-Sik Lee, “Recent developments in non-Fermi liquid theory,” Annu. Rev. Condens. Matter Phys. **9**, 227–244 (2018).
 - [3] Louis Taillefer, “Scattering and pairing in cuprate superconductors,” Annu. Rev. Condens. Matter Phys. **1**, 51–70 (2010).
 - [4] Bernhard Keimer, Steven A Kivelson, Michael R Norman, Shinichi Uchida, and J Zaanen, “From quantum matter to high-temperature superconductivity in copper oxides,” Nature **518**, 179–186 (2015).
 - [5] Qimiao Si and Frank Steglich, “Heavy fermions and quantum phase transitions,” Science **329**, 1161–1166 (2010).
 - [6] Yaroslav Tserkovnyak, Arne Brataas, and Gerrit E. W. Bauer, “Enhanced gilbert damping in thin ferromagnetic films,” Phys. Rev. Lett. **88**, 117601 (2002).
 - [7] Yaroslav Tserkovnyak, Arne Brataas, Gerrit E. W. Bauer, and Bertrand I. Halperin, “Nonlocal magnetization dynamics in ferromagnetic heterostructures,” Rev. Mod. Phys. **77**, 1375–1421 (2005).
 - [8] Yuichi Ohnuma, Hiroto Adachi, Eiji Saitoh, and Sadamichi Maekawa, “Enhanced dc spin pumping into a fluctuating ferromagnet near T_C ,” Phys. Rev. B **89**, 174417 (2014).
 - [9] M. Matsuo, Y. Ohnuma, T. Kato, and S. Maekawa, “Spin current noise of the spin seebeck effect and spin pumping,” Phys. Rev. Lett. **120**, 037201 (2018).
 - [10] T. Kato, Y. Ohnuma, M. Matsuo, J. Rech, T. Jonckheere, and T. Martin, “Microscopic theory of spin transport at the interface between a superconductor and a ferromagnetic insulator,” Phys. Rev. B **99**, 144411 (2019).
 - [11] MA Silaev, “Finite-frequency spin susceptibility and spin pumping in superconductors with spin-orbit relaxation,” Physical Review B **102**, 144521 (2020).
 - [12] Yuya Ominato, Ai Yamakage, and Mamoru Matsuo, “Anisotropic superconducting spin transport at magnetic interfaces,” Phys. Rev. B **106**, L161406 (2022).
 - [13] Wei Han, Sadamichi Maekawa, and Xin-Cheng Xie, “Spin current as a probe of quantum materials,” Nature Materials **19**, 139–152 (2019).
 - [14] Zhiyong Qiu, Jia Li, Dazhi Hou, Elke Arenholz, Alpha T N’Diaye, Ali Tan, Ken-ichi Uchida, Koji Sato, Satoshi Okamoto, Yaroslav Tserkovnyak, *et al.*, “Spin-current probe for phase transition in an insulator,” Nature communications **7**, 12670 (2016).
 - [15] Yuya Ominato, Ai Yamakage, Takeo Kato, and Mamoru Matsuo, “Ferromagnetic resonance modulation in d-wave superconductor/ferromagnetic insulator bilayer systems,” Physical Review B **105**, 205406 (2022).
 - [16] L. P. Gorkov A. A. Abrikosov and I. Y. Dzyaloshinskii, “Quantum field theoretical methods in statistical physics,” (1975).
 - [17] Qimiao Si, Rong Yu, and Elihu Abrahams, “High-temperature superconductivity in iron pnictides and chalcogenides,” Nature Reviews Materials **1** (2016), 10.1038/natrevmats.2016.17.
 - [18] Max A. Metlitski and Subir Sachdev, “Quantum phase transitions of metals in two spatial dimensions. i. ising-nematic order,” Phys. Rev. B **82**, 075127 (2010).
 - [19] Subir Sachdev, *Quantum Phase Transitions* (Cambridge University Press, 2011) Chap. 18.
 - [20] John A. Hertz, “Quantum critical phenomena,” Phys. Rev. B **14**, 1165–1184 (1976).
 - [21] A. J. Millis, “Effect of a nonzero temperature on quantum critical points in itinerant fermion systems,” Phys. Rev. B **48**, 7183–7196 (1993).
 - [22] See Supplemental Materials for a self-contained review of the NFL metal near the 2D Ising nematic QCP and detailed calculations.
 - [23] Luca Dell’Anna and Walter Metzner, “Fermi surface fluctuations and single electron excitations near pomeranchuk instability in two dimensions,” Phys. Rev. B **73**, 045127 (2006).
 - [24] Matthias Punk, “Finite-temperature scaling close to ising-nematic quantum critical points in two-dimensional metals,” Phys. Rev. B **94**, 195113 (2016).
 - [25] A. Liam Fitzpatrick, Shamit Kachru, Jared Kaplan, and S. Raghu, “Non-Fermi-liquid behavior of large- N_B quantum critical metals,” Phys. Rev. B **89**, 165114 (2014).
 - [26] Yoni Schattner, Samuel Lederer, Steven A. Kivelson, and Erez Berg, “Ising nematic quantum critical point in a metal: A monte carlo study,” Phys. Rev. X **6**, 031028 (2016).